

# Frequent disturbances enhanced the resilience of past human populations

**Philip Riris** (✉ [priris@bournemouth.ac.uk](mailto:priris@bournemouth.ac.uk))

Institute for Modelling Socio-Environmental Transitions <https://orcid.org/0000-0003-4244-7495>

**Fabio Silva**

Bournemouth University <https://orcid.org/0000-0003-1368-6331>

**Enrico Crema**

University of Cambridge <https://orcid.org/0000-0001-6727-5138>

**Alessio Palmisano**

3. Department of Historical Studies, University of Turin <https://orcid.org/0000-0003-0758-5032>

**Erick Robinson**

4. Native Environment Solutions; Native Environment Solutions LLC

**Peter Siegel**

5. Department of Anthropology, Montclair State University

**Jennifer French**

6. Department of Archaeology, Classics, and Egyptology, University of Liverpool

**Erlend Kirkeng Jørgensen**

7. NIKU High North Department, Norwegian Institute for Cultural Heritage Research

**S. Yoshi Maezumi**

Max Planck Institute of Geoanthropology <https://orcid.org/0000-0002-4333-1972>

**Steinar Solheim**

The Museum of Culture History, University of Oslo

**Jennifer Bates**

10. Department of Archaeology & Art History, Seoul National University

**Benjamin Davies**

Department of Anthropology, Yale University

**Yongje Oh**

10. Department of Archaeology & Art History, Seoul National University

**Xiaolin Ren**

12. Institute for the History of Natural Sciences, Chinese Academy of Sciences

---

**Social Sciences - Article**

**Keywords:**

**Posted Date:** December 11th, 2023

**DOI:** <https://doi.org/10.21203/rs.3.rs-3716011/v1>

**License:**  This work is licensed under a Creative Commons Attribution 4.0 International License.

[Read Full License](#)

**Additional Declarations:** There is **NO** Competing Interest.

---

# Abstract

The record of past human adaptations provides crucial lessons for guiding responses to crises in the future. To date, there have been no systematic global comparisons of humans' ability to absorb and recover from disturbances through time. We present results of the first attempt to synthesise resilience across a broad sample of prehistoric population time frequency data, spanning 30,000 years of human history. Cross-sectional and longitudinal analysis of population decline show that frequent disturbances enhance a population's capacity to resist and recover from later downturns. Land use patterns are important mediators of the strength of this positive association: farming and herding societies are more vulnerable but also more resilient overall. The results show that important trade-offs exist when adopting novel or alternate land use strategies.

# Main Text

Understanding the range of past responses of human societies to disturbances is a global priority across the social and natural sciences and will support the development of solutions to future crises<sup>1-3</sup>. Numerous case studies have addressed past cultural collapse, transformation, and persistence, although debate surrounds how to best characterise these processes<sup>4</sup>. A major unresolved issue is the lack of comparability between cases of population resilience in the historical sciences<sup>5,6</sup>. Few studies explicitly model impacts, recovery, and adaptation, or formally account for long-term history, which contains important and previously overlooked variation within and between cultural or environmental settings. Furthermore, a tendency to narrowly focus on responses to extreme events in both natural and social systems<sup>7,8</sup> may overemphasise local or short-term adaptive success at the expense of understanding large-scale or long-term vulnerabilities<sup>4,9</sup>. A well-known example is the shift to a narrow marine diet among the Greenland Norse that initially offset the short-term risk of crop failure yet heightened societal vulnerability to longer-term North Atlantic cooling<sup>10</sup>. Here, we establish a global comparative approach to long-term resilience to identify the factors that structure the response of prehistoric populations to disturbances through time. The approach measures population capacity to withstand changes, as well as the rate of recovery following a disturbance through the common proxy of radiocarbon time-frequency data<sup>11,12</sup>. Disturbances are the inferred drivers of relative reductions in population or archaeological activity in prehistory, described variously as recessions, downturns, busts, negative deviations, or similar<sup>12-15</sup>, and form the focus of this study, using summed probability distributions of calibrated radiocarbon dates (SPDs). SPDs function as an index of relative levels of human activity, or population change, over time<sup>16,17</sup>. Population downturns are defined as periods when SPDs are significantly below expected growth trajectories in response to disturbances. Our efforts focus on two key questions: 1) how quickly do past populations recover after downturns? and: 2) what factors mediate past resistance and resilience to downturns?

To quantify patterns in population resistance-resilience, we performed a meta-analysis of 16 published study regions that used archaeological radiocarbon data to reconstruct regional palaeodemographic

trends (**Table S1**). Our approach trades specificity for a large-scale, comparative perspective while still accounting for variation between cases to focus on the emergent properties of the statistical analysis. Studies were reviewed based on three criteria: evidence for significant downturns, their scope, and the inclusion of radiocarbon datasets. A lack of any single criterion resulted in the exclusion of a study. Cases with no reported downturns were not included, nor were those whose scope was restricted to specific activities within a regional radiocarbon dataset, such as flint mining<sup>18</sup>. Where published data have been superseded by later compilations, dates were added from the People3k database<sup>19</sup>, a systematic compilation of cleaned radiocarbon dates, based on the geographical area of the original study. Our global sample of regions ranges from the Arctic to the tropics and spans 30,000 years of history (**Fig. 1A**). Population downturns were reproduced using our protocol (**Methods**) and resistance-resilience metrics (**Fig. 1B**) were collected on 154 periods of population downturn, with a median of 8.5 periods in each region (**Fig. 1C; Table S1-S2**). The numerical metrics collectively capture the severity, chronology, and frequency of periods of statistically significant population downturn. Disturbances were classified into both general categories and specific drivers according to the original studies and expert interpretation of regional social, cultural, and environmental history (**Table S3**). The broad category of land use and evidence for adaptive change during, or in the wake of, downturns were also recorded. The focus of this meta-analysis is to identify the factors governing the relative depth of downturns (Resistance) and the rate of recovery at their conclusion (Resilience). A suite of hierarchical linear mixed models was developed to test for significant associations between parameters while controlling for regional variability (**Methods**).

This approach to past resistance-resilience provides a glimpse into population-level responses to disturbances throughout human history. Results demonstrate that a single factor – the frequency of downturns – increases both the ability to withstand disturbances, and to recover from them. Additionally, the frequency of downturn experienced by a given population is influenced by land use: agricultural and agropastoral populations experience significantly more downturns over time than other land use patterns recorded during downturns (**Table S3**). These findings collectively suggest that the global shift to food-producing economies during the Holocene (starting 11,700 calendar years Before Present) may have increased population vulnerability to disturbances, yet in the process enhanced their adaptive capacity through repeated exposure. Parallels to our long-term perspective on human population change in macroecology suggest that comparative approaches in the historical sciences have the potential to generate profound insights into past human-environmental relationships on a broad scale.

**Table 1: Metrics and model parameters extracted from global case studies of past population downturns.** Detailed descriptions of resistance-resilience metrics are in the **Methods**.

Name	Description	Notes
<i>Parameters</i>		
Overall duration	Length of downturn, in calendar years before present	
$n_{\text{downturn}}$	Cumulative number of downturns in a region	
Time to minimum	Time to SPD minimum value, in calendar years before present	
$T_{\text{start}}$	Calendar year before present at start of downturn	
$T_{\text{end}}$	Calendar year before present at end of downturn	
$G_b$	Baseline SPD value at the start of a downturn	
$G_x$	Minimum SPD value during a downturn	<b>fig. S4</b>
$G_e$	SPD value at the end of a downturn	
<i>Independent</i>		
Resistance	The depth of a downturn relative to baseline conditions. Range: 0–1	$1 - \frac{2 \times  G_b - G_x }{ G_b  +  G_b - G_x }$
Resilience	Rate of recovery to baseline conditions, controlling for maximum impact of downturn. Range: -1–1	$\frac{2 \times  G_b - G_x }{ G_b - G_x  +  G_b - G_e } - 1$
<i>Dependent</i>		
Geographical information	Latitude, longitude, world region.	
Relative pace	The time to SPD minimum normalised by downturn duration. Range: 0–1	$\frac{\text{Time to minimum}}{\text{Overall duration}}$
Frequency of downturns (FD)	Cumulative number of downturns standardised by duration in calendar years, per millennium.	$\left(\frac{n_{\text{downturn}}}{\text{Duration}}\right) * 1000$
Category	Driver of disturbance.	
Type	Type of disturbance.	<b>table S3</b>
Land use	Dominant land use pattern.	
Change	Cultural changes over the interval of the downturn.	Boolean variable, with specific responses noted separately

## Results

The most common high-level driver of downturns, after those with a lack of evidence for a specific cause (Unclear,  $n = 65$ ), is Environmental ( $n = 48$ , 31%), followed by Mixed (Cultural-Environmental) ( $n = 33$ , 21%). The most common disturbance type is aridity in the Environmental category ( $n = 31$ ), followed by mobility ( $n = 20$ ) in the Cultural category. Only a third of recorded downturns have resistance values that drop more than 50% from pre-downturn activity levels ( $n = 53$ , 34.4%; **Fig. 2A**). Most downturns ( $n = 133$ , 86%) end before baseline relative population levels are attained, in other words, observed SPD values

are *lower* at the end of most downturns than at the pre-disturbance reference value. Resilience is relatively high across all cases (median = 0.64,  $n = 154$ ), with 40% ( $n = 63$ ) still attaining 90% of pre-downturn conditions by their end (**Fig. 2B**). Full returns to SPD baseline conditions are frequently interrupted by subsequent downturns. Downturns associated with Cultural drivers return the highest median resilience (0.74), while the median Mixed (Cultural-Environmental) resistance is highest at 0.79. Resistance (0.65) and resilience is lowest among climate-driven downturns (0.57). However, we do not find support for significant differences in either metric across disturbance categories (ANOVA, *Resistance*:  $F = 0.541$ ,  $p = 0.65$ ,  $df = 3$ ,  $n = 154$ ; *Resilience*:  $F = 0.04$ ,  $p = 0.98$ ,  $df = 3$ ,  $n = 154$ ).

### ***Global variation in recovery rate***

Initial modelling indicates that the geographical location of downturns does not affect resistance, with the exceptions of significantly higher values in the Caribbean Archipelago and the Italian Peninsula. Conversely, there is support for significantly *lower* values for resilience in three regions: the Central China Plains, Caribbean Archipelago, and the Korean Peninsula, when compared to all other regions (**Table S4**). Further examination of these cases reveals that a large minority of downturns in these three regions return negative values of resilience ( $n = 11$ , 39%), which are produced when the population proxy *exceeds* the SPD value at the start of the downturn by its end (**Fig. S4, 12**). Although the SPD population proxy remains below modelled expectations in all these cases and are therefore in the strictest sense downturns relative to the null models, the results nevertheless imply that populations in these regions were, on average, able to recover faster than the norm. Due to the observed range of variation and its potential impact on the metrics, Study Region was retained as a random effect variable in the mixed-effect models.

### ***Long-term downturns are the norm***

The durations of population downturns tend towards centennial (100-500 years,  $n = 48$ , 31%) and decadal periods ( $\leq 50$  years,  $n = 47$ , 30.5%), with a median of 98 years across the sample. Downturns lasting longer than 500 years are a minority ( $n = 29$ ). The time taken to reach SPD minima skews further towards decadal timescales (**Fig. 2C**). Only a single downturn that commences with the 8.2ka event in the Near East<sup>20</sup> has a time to minimum longer than a millennium (2070 years). Both variables have a strong positive skew (Duration = 2.84, Time to minimum = 4.23). To control for the distribution and broad range of variation in these variables, the time to minimum is normalised by downturn duration to produce an index of its relative speed, which we term "Pace", **Fig. 2D**). This transformation enables comparison of the variation between downturns, with higher numbers reflecting slower downturns ( $\sigma = 0.55$ , s.d. = 0.23), and lacking support for non-normally distributed values as in the time to minimum and duration variables (Shapiro-Wilk  $W = 0.98396$ ,  $p = 0.07108$ ). Consequently, relative pace is employed as a fixed effect candidate in the mixed-effect modelling.

### ***Land use mediates resilience***

The frequency of downturns over time by region (FD) was estimated by normalising the cumulative number of downturns in a region by their duration (**Table 1**). We transform this to the logarithm of events

per millennium to account for its strongly skewed distribution. The variable allows us to compare the rate at which downturns occur. It consistently displays the strongest relationship to both resistance and resilience ( $p < 0.001$  in both cases, **Table S5**) and is the only fixed variable retained by the information criterion-based selection procedure.

Collectively, these results indicate that populations experience an enhanced ability to withstand disturbances as frequency increases, as well as to recover in the aftermath (**Figs. 3A-B**). Further examination of FD shows that, among the recorded disturbance types, changes to mobility regimes (median FD = 2.26,  $n = 20$ ) and high environmental variability (median FD = 2.19,  $n = 17$ ) occur at the highest rate per millennium, while cooling occurs at the lowest rate (median FD = 0.761,  $n = 4$ ) (**Fig. 3C**). In terms of regional variation, the highest frequency of downturn is recorded in the South African Greater Cape Floristic Region (median FD = 2.41,  $n = 17$  over 9950 years), and the lowest in the Korean Peninsula (median FD = 0.58,  $n = 3$  over 4000 years).

Treating the frequency of downturn (FD) as a response variable (**Methods**) reveals that agricultural and agropastoralist land use patterns are associated with significantly higher rates of downturn compared to low-level food production, marine foraging, or mixed subsistence. Results from this additional modelling exercise suggest that FD likely has an important effect on resistance and recovery, while FD itself covaries with the dominant pattern of land use and disturbance type in a given time and place. A larger sample size of downturns would increase the explanatory power of our approach and enhance our characterisation of these relationships.

## Discussion

This meta-analysis has examined the potential factors influencing resistance and resilience across a broad archaeological sample, while controlling for regional variation. The frequency of downturns is the main determinant of the observed outcomes, among the examined factors. The relationship between resistance and resilience displays variable rates, yet these events all tend to unfold at multidecadal to centennial timescales. Well-known historical examples support this finding: Indigenous depopulation across the Americas following European colonisation, though catastrophic, took centuries<sup>21</sup>, while the collapse of imperial power in Western Rome was preceded by a long period of rural depopulation<sup>22</sup>. Systematic data on independent population downturns in prehistory are less common, however, what is available<sup>23,24</sup> corroborates this result: palaeodemographic downturns resolved in radiocarbon data tend to last at least one human generation but frequently much longer.

The frequency of downturns (FD) is associated with both the ability of past populations to withstand downturns and the rate of recovery following them across a broad sample of human populations. This runs counter to the historical particularism of archaeological work on past resilience<sup>5,9</sup>, which often emphasises the contingencies, decisions, and practices that underwrote successful adaptations in specific times and places<sup>25,26</sup>. The results suggest the existence of a single common mechanism among human populations that confers resilience to disturbances. The size of this interaction is greater for

resistance ( $\eta^2 = 0.46$ ,  $p < 0.001$ , **Fig. 3B**) than resilience ( $\eta^2 = 0.29$ ,  $p < 0.001$ , **Fig. 3A**). In practical terms, this suggests that the ability to withstand downturns is distinct from the ability to recover in their wake. We note that this result does not imply a monocausal or deterministic relationship; there are likely to be multiple adaptive pathways that increase population resistance and resilience via the mechanism of increasing disturbance frequency.

Further testing indicates that land use practices associated with food production, such as farming and herding, are significantly and positively correlated with the frequency of downturns (**Table S5, Fig. 3C**). From the early Holocene, the proportion of land use associated with food production in our sample of downturns also increases, as the aggregate global population becomes gradually more reliant on domesticated species for meeting subsistence needs (**Fig. 3D**). Collectively, these trends show that while populations generally increased resistance and resilience over time, the heightened rate of downturn (FD) over time is itself likely linked to the historical tendency towards food producing subsistence systems. Current archaeological evidence does not indicate that this process was unidirectional or inevitable; foraging and food production are neither mutually exclusive nor in opposition. Our synthetic findings agree with specific cases showing that the behavioural and social changes food production entailed had trade-offs in other arenas<sup>23</sup>.

Traditional agricultural or agropastoral practices include a diverse range of socio-ecological systems that are often highlighted as potential sources of inspiration for solutions to current sustainability, biodiversity, and conservation challenges<sup>6,10,27,28</sup>. The results suggest that population downturns or collapse are an inherent property of these systems and a potential trade-off of promoting their use. Systematic reviews in disturbance ecology indicate that frequent natural disturbances enhance the long-term resilience of key ecosystem services, and that localised, subsystem declines are an important mechanism through which this occurs<sup>29</sup>. Our study provides insight into the possible existence of an analogous relationship within our sample of human populations; higher frequencies are strongly correlated to both smaller downturns and closer matches to pre-downturn values in the SPD proxies. We suggest that humanity's overall constant long-term population growth<sup>30</sup> may have been sustained in part due to the emergent positive feedback between vulnerability, resistance, and recovery documented here.

Population decline has been termed an 'inevitable' feature of our species' demographic dynamics<sup>31</sup>. In their systematic review of historical collapse and resilience dynamics, Cumming and Peterson<sup>1</sup> list depopulation as a key metric or factor in every ancient socio-ecological system studied. We anticipate this singular status will continue undiminished. Our contribution indicates that downturns play an important role in human population history by enhancing the resilience of survivor populations. We speculate that the creation of biased cultural transmission is responsible, however, this potential causal link needs to be rigorously tested. Population downturns have been identified as potential triggers of labour investment in infrastructure, social cohesion, and technological advancement<sup>15</sup>. Together, these mechanisms have the potential to enhance the preferential transmission of knowledge and practices that promote future resistance or resilience<sup>10</sup>. Raising population thresholds by intensifying land use may



also heighten the risk of more serious collapse in return for increasingly marginal benefits<sup>1,24,32</sup>. Other non-trivial and historically contingent factors that likely affect outcomes are the diversity and ecology of domesticated species assemblages, degree and type of political complexity, and settlement patterning in relation to the environment. Indicators such as the cessation of monument construction, loss of literacy, or economic turmoil can provide additional insight around the consequences and/or potential drivers of population downturns. As a first attempt at a comparative analysis of palaeodemographic resistance-resilience, however, our analysis does not distinguish between these elements of the populations under study.

This study finds parallels in macroecology, where analogous resistance-resilience outcomes have been suggested to only fully resolve at centennial time scales or above<sup>33,34</sup>. Archaeology is uniquely suited to examining past population history – and the dynamics that underlie these trends – at such long-term time scales<sup>35,36</sup>. Understanding past societies' responses to crises is often explicitly motivated by the goal of applying learnings from the historical sciences to present-day policy and activism, contributing to the ultimate objective of fostering resilient adaptations for the future<sup>4</sup>. We argue that a prerequisite for the historical sciences to play this role is an improved understanding of the processes and drivers that influence long-term, centennial-scale resilience<sup>6</sup>. Our approach has for the first time highlighted the global relationship between population change and frequency of disturbance over millennial timescales, and which applies across a broad geographical and chronological sample of past populations, including prehistoric examples that are overlooked in systematic reviews of societal resilience more broadly. Improved clarity on the drivers of exposure frequency and type in the past will help reveal the mechanism(s) behind the dynamics we describe and their potential limits, particularly important as environmental variability is predicted to increase in the future<sup>37,38</sup>. Archaeological and historical case studies have focused on the frequency of volcanism, warfare<sup>39</sup>, and hydroclimatic oscillations<sup>23,40</sup>, as well as the rate of abrupt or extreme events in general<sup>8</sup>. Comparable evidence on different categories of downturns is necessary. Synthesis of these or similar data in a comparative framework can provide important insights into the causal links between population resilience, risk of exposure, and ultimately, the ability to recover.

## Declarations

### Funding:

Samsung Electronics Co., Ltd. Grant A0342-20220007 (JB)

Leverhulme Trust grant #PLP-2019–304 (EC)

The Youth Innovation Promotion Association of the Chinese Academy of Sciences grant YIPA-CAS, 2022149 (XR)

### Author Contribution statement:

Conceptualization: PR, FS

Methodology: PR, EC, AP, FS

Investigation: PR, BD, EKJ, YO, AP, XR, ER, PS, SS

Analysis: PR, EC, FS

Writing: PR, JCF, PS

Editing: PR, JB, EC, JCF, EKJ, SYM, AP, ER, PS, FS, SS

Visualization: PR, SYM, ER

**Competing Interests:** Authors declare that they have no competing interests.

Supplementary Information is available for this paper. Correspondence and request for material should be addressed to PR.

### **Data availability statement**

The data and code that support the findings of this study are available in Zenodo with the identifier doi: 10.5281/zenodo.10061467 (<https://dx.doi.org/10.5281/zenodo.10061467>).

## **References**

1. Cumming, G.S., G.D. Peterson. Unifying research on social–ecological resilience and collapse. *Trends Ecol. Evol.* **32**, 695–713 (2017).
2. Haldon, J., L. Mordechai, T.P. Newfield, A.F. Chase, A. Izdebski, P. Guzowski, I. Labuhn, N. Roberts, History meets palaeoscience: Consilience and collaboration in studying past societal responses to environmental change. *Proc. Natl. Acad. Sci. U.S.A.* **115**, 3210–8 (2018).
3. IPBES, *Global assessment report on biodiversity and ecosystem services of the Intergovernmental Science-Policy Platform on Biodiversity and Ecosystem Services* (IPBES secretariat, 2019). <https://doi.org/10.5281/zenodo.3831673>
4. Degroot, D. et al. Towards a rigorous understanding of societal responses to climate change. *Nature* **591**, 539–50 (2021).
5. Bradtmöller, M., S. Grimm, J. Riel-Salvatore, Resilience theory in archaeological practice—An annotated review. *Quat. Int.* **446**, 3–16 (2017).
6. Silva, F. et al., Developing transdisciplinary approaches to sustainability challenges: The need to model socio-environmental systems in the *longue durée*. *Sustainability* **14**, 10234 (2022).
7. Broska, L.H., W.R. Poganietz, S. Vögele, Extreme events defined—A conceptual discussion applying a complex systems approach. *Futures* **1**, 102490 (2020).

8. Pausas, J.G., A.B. Leverkus, Disturbance ecology in human societies. *People Nat.***5**, 1082-1093 (2023).
9. Middleton, G.D. The show must go on: collapse, resilience, and transformation in 21st-century archaeology. *Rev. Anthropol.* **46**, 78-105 (2017).
10. Jackson, R.C., A.J. Dugmore, F. Riede, Rediscovering lessons of adaptation from the past. *Glob. Environ. Change***52**, 58-65 (2018).
11. Van Meerbeek, K., T. Jucker, J.C. Svenning, Unifying the concepts of stability and resilience in ecology. *Journal of Ecology***109**, 3114-32 (2021).
12. Riris, P., J.G. De Souza, Formal tests for resistance-resilience in archaeological time series. *Front. Ecol. Evol.***9**, 740629 (2021). doi: 10.3389/fevo.2021.740629
13. Shennan, S. et al. Regional population collapse followed initial agriculture booms in mid-Holocene Europe. *Nat. Commun.***4**, 2486 (2013).
14. Bevan, A. et al. Holocene fluctuations in human population demonstrate repeated links to food production and climate. *Proc. Natl. Acad. Sci. U.S.A.* **114**, E10524-31 (2017).
15. Freeman, J., R.P. Mauldin, M. Whisenhunt, R.J. Hard, J.M. Anderies, Repeated long-term population growth overshoots and recessions among hunter-gatherers. *The Holocene* **7**, 09596836231183072 (2023).
16. Freeman, J., D.A. Byers, E. Robinson, R.L. Kelly, Culture process and the interpretation of radiocarbon data. *Radiocarbon***60**, 453-67 (2018).
17. Crema, E.R., A. Bevan, Inference from large sets of radiocarbon dates: software and methods. *Radiocarbon***63**, 23-39 (2021). doi: 10.1017/RDC.2020.95
18. Schauer, P. et al. Supply and demand in prehistory? Economics of Neolithic mining in northwest Europe. *J. Anthropol. Archaeol.***54**, 149-60 (2019).
19. Bird, D. et al. p3k14c, a synthetic global database of archaeological radiocarbon dates. *Sci. Data.* **27**, 27 (2022).
20. Palmisano, A., D. Lawrence, M.W. de Gruchy, A. Bevan, S. Shennan. Holocene regional population dynamics and climatic trends in the Near East: A first comparison using archaeo-demographic proxies. *Quat. Sci. Rev.***252**, 106739 (2021).
21. Koch, A., C. Brierley, M.M. Maslin, S.L. Lewis. Earth system impacts of the European arrival and Great Dying in the Americas after 1492. *Quat. Sci. Rev.***207**, 13-36 (2019).
22. Storey, R., G.R. Storey, *Rome and the Classic Maya: Comparing the slow collapse of civilizations.* (Routledge, 2017).
23. Finley, J.B., E. Robinson, R.J. DeRose, E. Hora. Multidecadal climate variability and the florescence of Fremont societies in Eastern Utah. *American Antiquity***85**, 93-112 (2020).
24. Freeman, J. et al., Landscape engineering impacts the long-term stability of agricultural populations. *Hum. Ecol.***49**, 369-82 (2021).

25. Allen, K.J. et al. Coupled insights from the palaeoenvironmental, historical and archaeological archives to support social-ecological resilience and the sustainable development goals. *Environ. Res. Lett.***17**, 055011 (2022).
26. Schug, G.R. et al. Climate change, human health, and resilience in the Holocene. *Proc. Natl. Acad. Sci. U.S.A.***120**, e2209472120 (2023). doi: 10.1073/pnas.2209472120
27. Boivin, N., A. Crowther, Mobilizing the past to shape a better Anthropocene. *Nat. Ecol. Evol.***5**, 273-84 (2021).
28. Burke, A. et al., The archaeology of climate change: The case for cultural diversity. *Proc. Natl. Acad. Sci. U.S.A.***118**, e2108537118 (2021).
29. Seidl, R., W. Rammer, T.A. Spies, Disturbance legacies increase the resilience of forest ecosystem structure, composition, and functioning. *Ecol. Appl.* **24**, 2063-77 (2014).
30. Zahid, H.J., E. Robinson, R.L. Kelly. Agriculture, population growth, and statistical analysis of the radiocarbon record. *Proc. Natl. Acad. Sci. U.S.A.***113**, 931-5 (2016).
31. Shennan, S., R. Sear. Archaeology, demography and life history theory together can help us explain past and present population patterns. *Philos. Trans. R. Soc. Lond., B, Biol. Sci.***376**, 20190711 (2021).
32. De Souza, J.G. et al. Climate change and cultural resilience in late pre-Columbian Amazonia. *Nat. Ecol. Evol.***3**, 1007-17 (2019).
33. Cole, L.E., S.A. Bhagwat, K.J. Willis, Recovery and resilience of tropical forests after disturbance. *Nat. Commun.* **20**, 3906 (2014).
34. Cant, J., P. Capdevila, M. Beger, R. Salguero-Gómez, Recent exposure to environmental stochasticity does not determine the demographic resilience of natural populations. *Ecol. Lett.***26**, 1186-99 (2023). doi: 10.1111/ele.14234
35. Redman, C.L. Resilience theory in archaeology. *Am. Anthropol.***107**, 70-7 (2005).
36. French, J.C., P. Riris, J. Fernandez-Lopez de Pablo, S. Lozano, F. Silva, A manifesto for palaeodemography in the twenty-first century. *Philos. Trans. R. Soc. Lond., B, Biol. Sci.***376**, 20190707 (2021).
37. Wisner, A., P. Blaikie, T. Cannon, I. Davis, *At risk: Natural Hazards, People's Vulnerability and Disasters*. (Routledge, 2014).
38. Thornton, P.K., P.J. Ericksen, M. Herrero, A.J. Challinor, Climate variability and vulnerability to climate change: a review. *Glob. Change Biol.* **20**, 3313-28 (2014).
39. Gao, C. et al. Volcanic climate impacts can act as ultimate and proximate causes of Chinese dynastic collapse. *Commun. Earth Environ.***2**, 234 (2021).
40. Douglas, P.M., A.A. Demarest, M. Brenner, M.A. Canuto, Impacts of climate change on the collapse of lowland Maya civilization. *Annu. Rev. Earth Planet Sci.***44**, 613-45 (2016).

## Methods

### *Calibration and aggregation*

Archaeological radiocarbon dates were collated from published studies that previously adopted null hypothesis significance testing (NHST) approaches towards prehistoric demography. Our literature search identified 16 studies that collectively span six continents and approximately 30,000 radiocarbon years (**table S1**). We applied a consistent protocol to the calibration of radiocarbon assays. The *calibrate* function within the R package *rcarbon*<sup>17</sup> was used to convert <sup>14</sup>C radiocarbon years to calendar years before present (cal BP). The IntCal20<sup>41</sup> and SHCal20<sup>42</sup> curves were applied to dates in the northern and southern hemispheres, respectively. Calibrated ages are reported as the 95.4% (two-sigma, 2 $\sigma$ ) age range. Laboratory codes and Site Identification numbers were appended to each calibrated date range and post-calibration distributions were not normalised. To account for between-site variation in sampling intensity, multiple dates from a single site that are within 50 radiocarbon years of each other were pooled ('binned') before aggregation into regional summed probability distributions (SPDs).

### ***Bayesian model fitting***

Our protocol aims to replicate the results of the 16 identified case studies to the greatest extent possible. In order to reproduce statistically significant negative population events ('downturns') produced by *rcarbon*'s 'modelTest()' function in the original studies, while simultaneously addressing the well-known limitations of using summed probability distributions in NHST, we adopt an alternative, Bayesian modelling approach. Markov Chain Monte Carlo (MCMC) methods implemented in the *nimbleCarbon* package<sup>43</sup> for radiocarbon data can obtain robust parameter estimates, as the Bayesian MCMC controls for radiocarbon measurement errors and sampling biases separately. Previously, this has been a major drawback of NHST approaches to aggregated radiocarbon data, with several alternatives proposed in the literature<sup>44,45</sup>. Using the MCMC-derived parameter estimates in posterior predictive checks enables us to detect periods where expected growth trajectories are lower than the fitted model parameters, and which are more robust than least-squares regression approaches. The protocol produces outputs that are analogous to those in prior NHST studies (**Figure S**).

We analyse regional SPDs separately by fitting identical bounded exponential growth models to each dataset. This common model is defined by three parameters: growth rate ( $r$ ) and boundaries ( $a$  and  $b$ ). A weakly informative exponentially distributed prior ( $\lambda = 1/000.4$ ) was used for  $r$  to capture a broad range of potential growth rates among the cases. Parameters  $a$  and  $b$  were adopted from the original studies. Markov chain traceplots (**Figure S-Figure S**) evaluate chain mixing alongside model convergence (Gelman-Rubin  $\hat{R}$ ) and effective sample size (ESS) diagnostics (**table S7**). Three chains of 50,000 iterations were run per region, with a burn-in of 5000 iterations and a thinning interval of 2. To ensure comparability of results with published studies that used a logistic growth model as a null hypothesis, regional datasets were subset based on expert judgement at documented palaeodemographic transitions and treated as two separate exponential growth models. Subsetting was only performed on the Near East and Italy, Sicily, and Sardinia datasets. Downturns adjacent to transition points were removed from the sample to avoid including data points introduced by the subsetting. Posterior predictive checks were executed using samples of parameter estimates obtained by the MCMC approach to simulate and back-

calibrate a number of radiocarbon dates equal to the sample size. The procedure was repeated 1000 times to derive critical envelopes.

### ***Resilience metrics***

The resilience metrics target periods where empirical SPD curves are below the 90% confidence envelopes of the fitted models, per the posterior predictive checks (periods termed 'downturns'). Extraction was performed using a bespoke R function modified from Riris and De Souza<sup>12</sup>, available in the repository (<https://dx.doi.org/10.5281/zenodo.10061467>). The principal response metrics in our analysis are Resistance and Resilience (**Figure S4**). Respectively, these metrics quantify the normalised response to downturns and the rate of recovery relative to baseline conditions. Resistance is measured on SPDs using two parameters: SPD values at the start of a downturn ( $G_b$ ) and at downturn minima ( $G_x$ ), while resilience is measured across the entire period of decline until its end ( $G_e$ ) relative to the minimum and baseline (**table 1**). Resistance ranges between 0 – 1, indicating a 100% change from baseline to no change. Resilience ranges between  $\pm 1$ , with 1 indicating full recovery by the end of the downturn. Negative values of resilience indicate that the baseline value has been exceeded, although remaining outside the expectations of the null model. Finally, zero indicates no recovery<sup>11,46</sup>. We also collected information on the start and ends of downturns, their duration, elapsed time until SPD minima were reached, and the cumulative number of recoveries (**table S2**).

### ***Statistical modelling***

The target of our comparative analysis is the resistance and resilience of human populations to disturbance as defined in each individual study. Our approach assumes that high values reflect resilient populations that successfully re-establish growth regimes after periods of decline related to disturbance events. We also assume that downturns are randomly distributed in time and geographical space. To account for the influence of inter-regional and -event cultural variation on outcomes, we drew on expert judgement and close readings of the published literature to record the broad category and specific type of disturbance during downturns, as well as the dominant land use type and the nature of resulting socio-cultural changes, if any (**table S3**). These variables provide a control on whether a given population within a cultural system retains its identity and function over time, or if system transformation and adaptive change is archaeologically evident.

Linear mixed-effect models were executed to evaluate the presence and strength of relationships between resistance, resilience, the recorded variables, and case study locations. This analysis was performed using the *cAIC4* and *lme4* R packages<sup>47,48</sup>, scripts are available in this repository: <https://dx.doi.org/10.5281/zenodo.10061467>. Initial models were defined with Resistance and Resilience as response variables, with only case identifiers (Region) as a random effect. As observed downturns are sequential within each case, the random effect controls for potential pseudoreplication while avoiding the need to weight the data by group size. A stepwise search using Akaike's Information Criterion was implemented for investigating the information gain of including fixed effects in each model in turn. These

candidate models were sequentially fitted using restricted maximum likelihood. Most fixed covariates (**Results, table S5**) were left out of the final models. Region was retained as a random effect in all cases, to produce two models:

$$\textit{Resistance} \sim (1|\textit{Region}) + \textit{Frequency of downturn}$$

$$\textit{Resilience} \sim (1|\textit{Region}) + \textit{Frequency of downturn}$$

Model output is summarised in **table S5** and diagnostics in **Figure S5-Figure S6**. We present standardised residuals, by region and in full, as well as leverage and Cook's Distance.

To further explore the relationship between rates of downturns and Resistance and Resilience, we performed an additional modelling exercise with the same random effect and full suite of fixed effects, with the frequency of downturn as the independent variable (**table S6, Figure S7**):

$$\textit{Frequency of downturn} \sim (1|\textit{Region}) + \textit{Land Use} + \textit{Change} + \textit{Disturbance Type} + \textit{Pace}$$

The effect sizes (standardised coefficients) of the significant model terms are plotted graphically in **fig. 4C** and reported in full in **table S6**. We report effect sizes in the text as  $\eta^2$  (eta-squared), that is, the total variance explained by differences between means.

## METHODS REFERENCES

41. Reimer, P.J. et al. The IntCal20 Northern Hemisphere radiocarbon age calibration curve (0–55 cal kBP). *Radiocarbon***62**, 725-57 (2020).
42. Hogg, A.G. et al. SHCal20 Southern Hemisphere calibration, 0–55,000 years cal BP. *Radiocarbon***62**, 759-78 (2020).
43. Crema, E.R. nimbleCarbon (v.0.2.1): Models and Utility Functions for Bayesian Analyses of Radiocarbon Dates with NIMBLE (2022). <https://github.com/ercrema/nimbleCarbon>.
44. Carleton, W.C. Evaluating Bayesian Radiocarbon-dated Event Count (REC) models for the study of long-term human and environmental processes. *J. Quat. Sci.***36**, 110-123 (2021).
45. Timpson, A., R. Barberena, M.G. Thomas, C. Méndez, K. Manning, Directly modelling population dynamics in the South American Arid Diagonal using  $^{14}\text{C}$  dates. *Philos. Trans. R. Soc. Lond., B, Biol. Sci.***376**, 20190723 (2021).
46. Orwin, K.H., D.A. Wardle, New indices for quantifying the resistance and resilience of soil biota to exogenous disturbances. *Soil Biol. Biochem.* **36**, 1907-1912 (2004).

47. Bates, D., M. Mächler, B. Bolker, S. Walker, Fitting Linear Mixed-Effects Models Using lme4. *J. Stat. Softw.* **67**, 1–48. (2015). doi:10.18637/jss.v067.i01.

48. Säfken, B., D. Rügamer, T. Kneib, S. Greven, Conditional Model Selection in Mixed-Effects Models with cAIC4. *J. Stat. Softw.* **99**, 1–30 (2021). doi:10.18637/jss.v099.i08.

## Figures

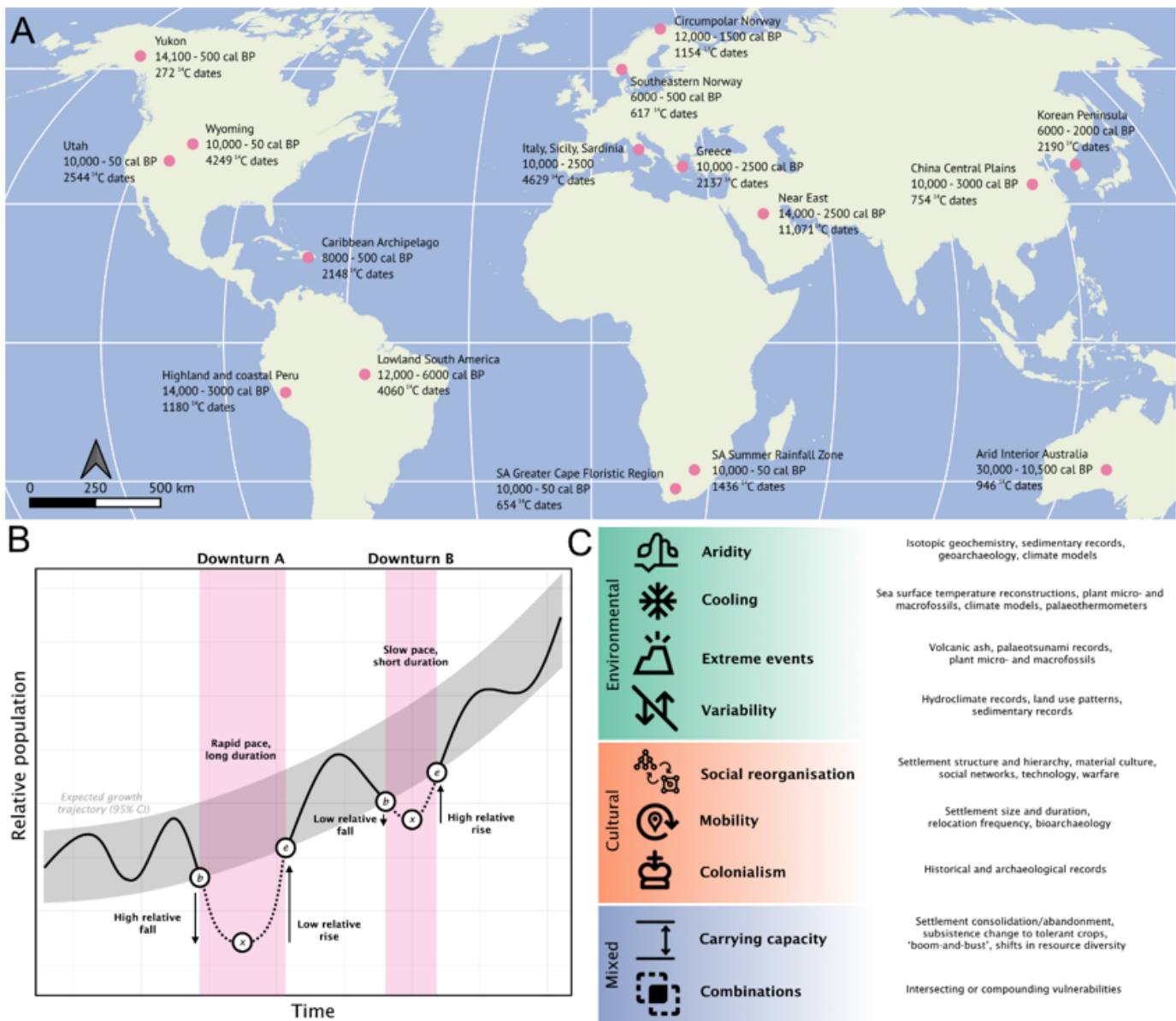
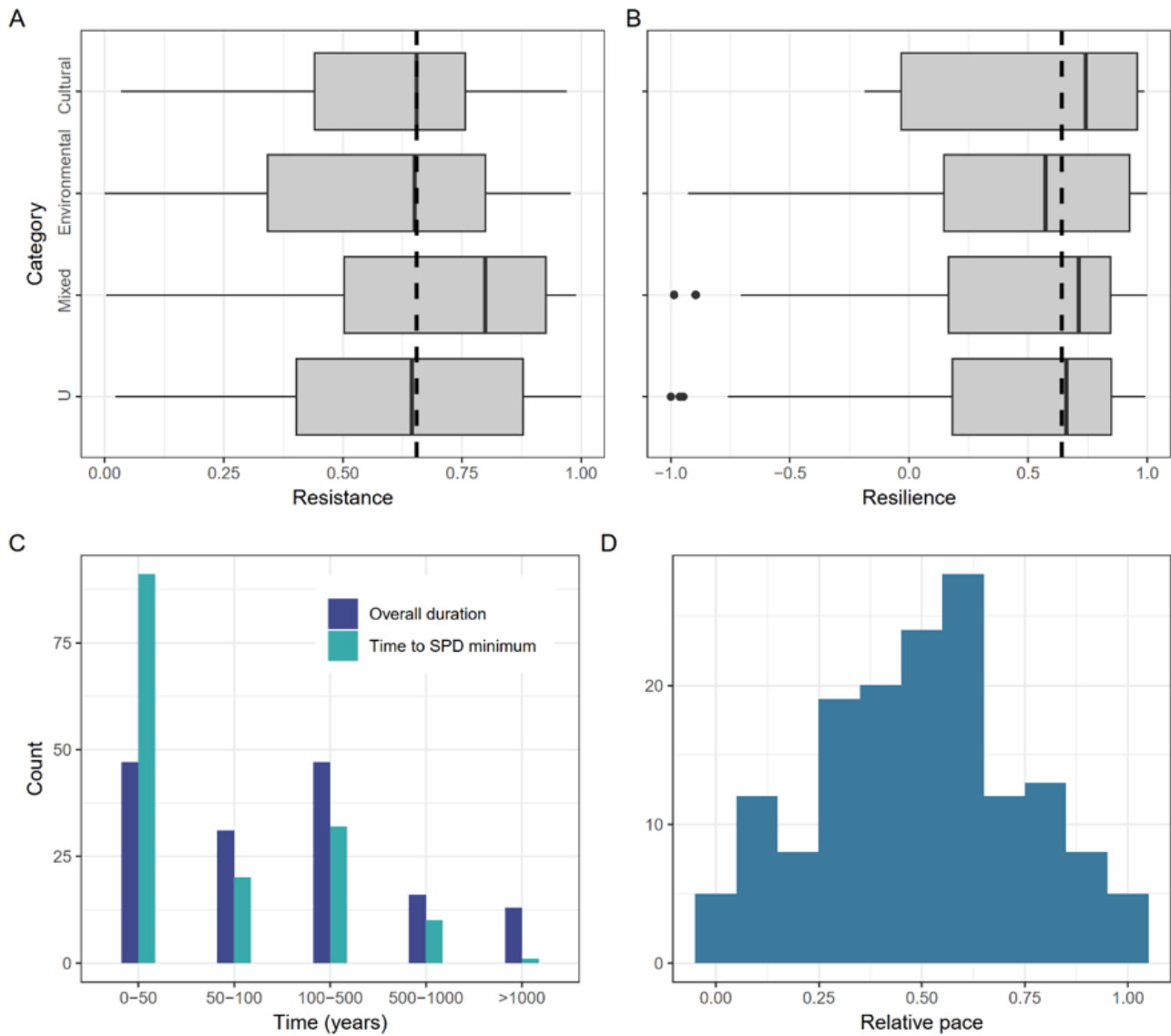


Figure 1

(A) World map of study regions. Time ranges and  $^{14}\text{C}$  dates used in this meta-analysis indicated for each region. (B) Conceptual diagram of measuring resistance-resilience on palaeodemographic downturns against expected growth trajectories. Downturn A is longer and faster, with low resistance and low relative



rate of recovery (resilience). Downturn B is shorter and slower, displaying higher resistance and higher resilience. Other combinations of high/low resistance and/or resilience are possible (Fig. S4). Parameters  $b$ ,  $x$ , and  $e$  for the equations in Table 1 are indicated in white dots. (C) Summary of disturbance types within three broad categories reported in published palaeodemographic studies. Listed proxies are examples drawn from the surveyed literature. “Unclear” (downturns with a lack of clear evidence for a driver) not shown (Table S3).



**Figure 2**

**Summaries of downturn numerical metrics.** Distributions of (A)resistance and (B) resilience across disturbance categories. Dashed line represents the data median. (C) Distribution of the duration of downturns and the time to SPD minima across all recorded downturns. (D) Relative pace (overall duration normalised by time to minimum) approximates a normal distribution and enables comparison of the

speed of downturns. Modelled downturn durations skew towards multidecadal and centennial time scales.

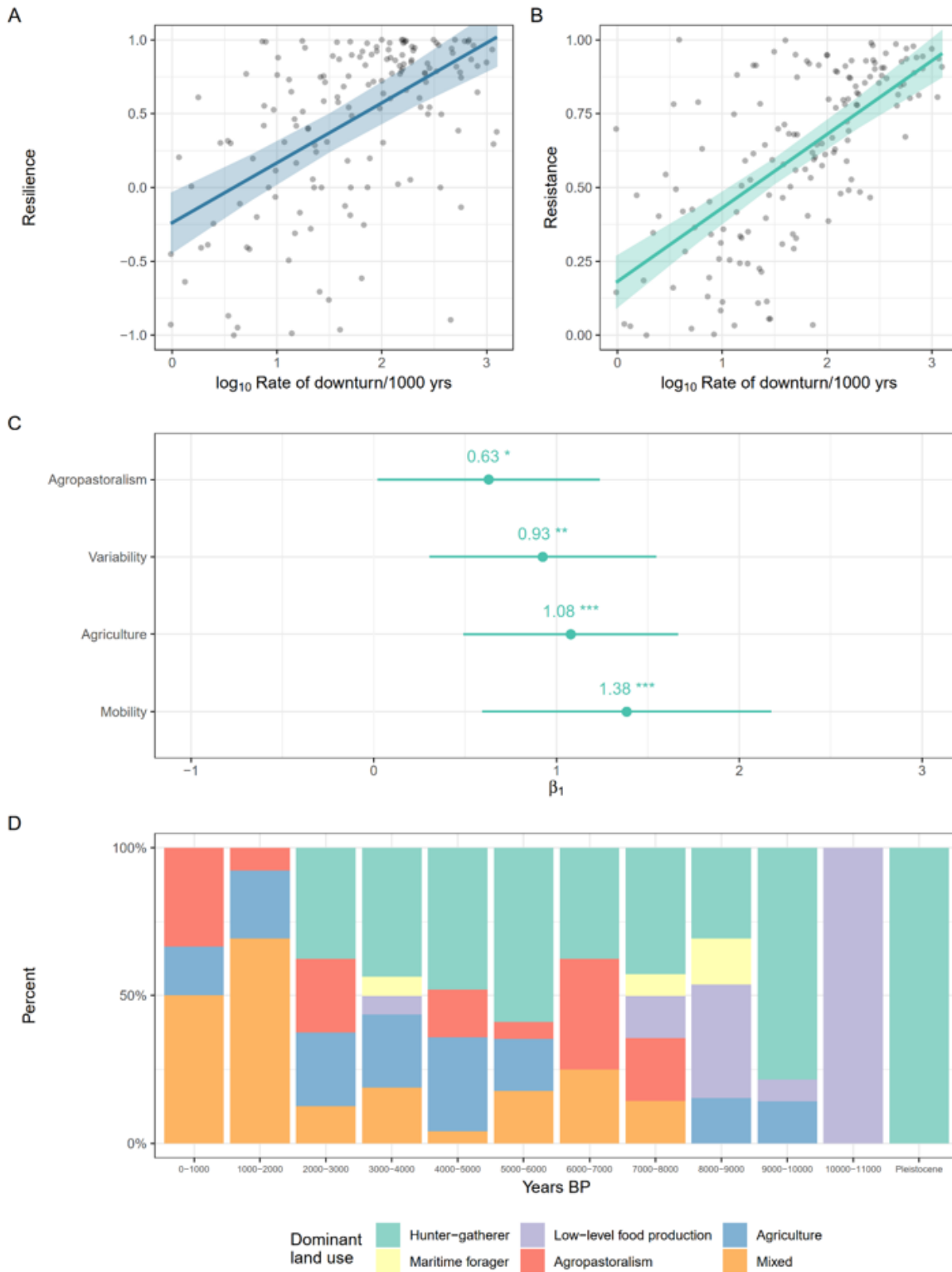


**Figure 3**

**Effect sizes of model terms and dominant land use during downturns.** Resilience (A) and Resistance (B) are strongly influenced by the rate of downturn per millennium, with a stronger effect for Resistance.

Values are extracted from fitted Models I & II. **(C)**Standardised regression coefficients for significant model terms. Hunter-gatherer was set as the reference group for land use. **(D)**Proportions of dominant land use types during downturns, in 1000-year time slices. Pleistocene downturns (before 11,000 calendar years Before Present, n = 24) have been combined.

## Supplementary Files

This is a list of supplementary files associated with this preprint. Click to download.

- [SupplementaryInformationformanuscriptX20231222116.docx](#)
- [EXTENDED DATA.docx](#)